Electrochemical and Ferromagnetic Couplings in 4,4′,4″-(1,3,5-Benzenetriyl)tris(phenoxyl) Radical Formation

Hiroyuki Nishide,* Ryuji Doi, Kenichi Oyaizu, and Eishun Tsuchida

Department of Polymer Chemistry, Waseda University, Tokyo 169-8555, Japan

nishide@mn.wasseda.ac.jp

Received September 5, 2000

4,4′,4″-(1,3,5-Benzenetriyl)tris(2,6-di-*tert*-butylphenol) was prepared by the cross-coupling of 1,3,5-tribromobenzene and [4-(trimethylsiloxy)phenyl]magnesium bromide. X-ray analysis of the single crystal showed a propeller-like structure with a mean dihedral angle of 39° between the hydroxyphenyl and the core benzene. The phenoxyl mono-, di-, and triradicals were generated by the electrochemical oxidation of the trianion. A stepwise radical formation was revealed by a differential pulse voltammogram, electrolytic ESR spectroscopy, and a comproportionation reaction between the radicals, which was discussed as an effect of the π-conjugated but non-Kekulé-type coupler. The quartet and triplet ground state for the tri- and diradical, respectively, were confirmed by a SQUID measurement.

Introduction

A 1,3,5-benzenetriyl unit has often been studied as one of the strongest π-conjugated couplers to ferromagnetically connect the spins of unpaired electrons of organic radical groups.[1] A variety of radical groups have been introduced to the 1,3,5-benzenetriyl core; e.g., 1,3,5-benzenetriyls tris-substituted with diarylmethyl,[2] nitronyl nitroxide,[3] *tert*-butyl nitroxide,[4] phenylcarbene,[5] and a diphenylamine cation radical.[6] The study of these 1,3,5-benzenetriyl-coupled radicals has been exhaustively continued to extend them to ferromagnetic organic polyradicals.[7] However, some of these organic radicals are not persistent under ambient conditions and/or the ferromagnetic interactions are not strong enough in magnitude. The exchange interaction and the chemical stability trade off for organic radicals: Among them, 2,6-di-*tert*-butylphenoxyl displays an intermediate property with adequate interaction and stability.

The 1,3,5-benzenetriyl combined with the phenoxyl, i.e., 4,4′,4″-(1,3,5-benzenetriyl)tris(2,6-di-*tert*-butylphenoxyl) (**1a**, Chart 1) and its precursor (**1b**) were first prepared by Zimmermann et al.:[8] **1a** was fairly stable, and their ESR study at 77K indicated the existence of a quartet state.[8,9] The corresponding biradical moiety, *m*-bis(3′,5′-di-*tert*-butyl-4-hydroxyphenyl)benzene (**2b**), was prepared by Mukai et al.: they described the triplet state of **2a** with ESR hyperfine structures.[10] On the other hand, we have succeeded in synthesizing poly(1,4- or 1,2-phenylenevinylene or -ethynylene)s that are pendantly 2- or 4-substituted with the 2,6-di-*tert*-butylphenoxyl group and in measuring an intramacromolecular ferromagnetic coupling between the spins of the pendant phenoxyls.[11] These results support the belief that the phenoxyl radical is an effective spin source to construct a ferromagnetic organic polymer. However, a quantitative generation of the phenoxyl radical combined with the π-conjugated couplers and the ferromagnetic spin inter-

Chart 1

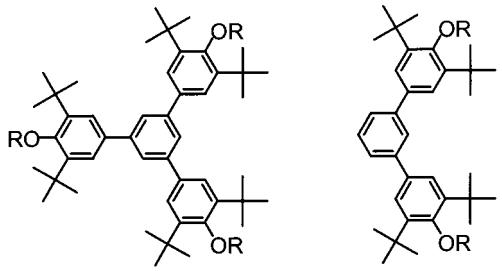

R = · **1a**
H **1b**
$Si(CH_3)_3$ **1c**

R = · **2a**
H **2b**

(1) (a) Dougherty, D. A. *Acc. Chem. Res.* **1991**, *24*, 88. (b) Iwamura, H.; Koga, N. *Acc. Chem. Res.* **1993**, *26*, 346. (c) Rajca, A. *Chem. Rev.* **1994**, *94*, 871. (d) Lahti, P. M. *Magnetic Properties of Organic Materials*; Marcel Dekker: New York, 1999.

(2) (a) Leo, M. *Berichte* **1937**, *70*, 1691. (b) Schmauss, G.; Baumgaerten, H.; Zimmermann, H. *Angew. Chem., Int. Ed. Engl.* **1965**, *4*, 596. (c) Sedo, J.; Ventosa, N.; Ruiz-Molina, D.; Rovira, C.; Veciana, J. *Angew. Chem., Int. Ed. Eng.* **1998**, *37*, 330.

(3) Dulog, L.; Kim, J. S. *Angew. Chem., Int. Ed. Engl.* **1990**, *29*, 415.

(4) Kanno, F.; Inoue, K.; Koga, N.; Iwamura, H. *J. Phys. Chem.* **1993**, *97*, 13267.

(5) Takui T.; Itoh, K. *Chem. Phys. Lett.* **1973**, *19*, 120.

(6) Yoshizawa, K.; Chano, A.; Ito, A.; Tanaka, K.; Yamabe, T.; Fujita, H.; Yamauchi, J.; Shiro, M. *J. Am. Chem. Soc.* **1992**, *114*, 5994.

(7) (a) Nakamura, N.; Inoue, K.; Iwamura, H. *Angew. Chem., Int. Ed. Engl.* **1993**, *32*, 872. (b) Matsuda, K.; Nakamura, N.; Inoue, K.; Koga, N.; Iwamura, H. *Bull. Chem. Soc. Jpn.* **1996**, *69*, 1483. (c) Rajca, A.; Lu, K.; Rajca, S. *J. Am. Chem. Soc.* **1997**, *119*, 10355. (d) Rajca, A.; Wongsriratanakul, J.; Rajca, S. *J. Am. Chem. Soc.* **1997**, *119*, 11674. (e) Bushby, R. J.; Gooding, D. *J. Chem. Soc., Perkin Trans. 2* **1998**, 1069. (f) Rajca, A.; Wongstriratanakul, J.; Rajca, S.; Cerny, R. *Angew. Chem., Int. Ed. Engl.* **1998**, *37*, 1229. (g) Rajca, A.; Rajca, S.; Wongstriratanakul, J. *J. Am. Chem. Soc.* **1999**, *121*, 6308.

(8) Kothe, G.; Nowak, C.; Denkel, K. H.; Ohmes, E.; Zimmermann, H. *Angew. Chem., Int. Ed. Engl.* **1970**, *9*, 520.

(9) Nowak, C.; Kothe, G.; Zimmermann, H. *Ber. Bunsen-Ges. Phys. Chem.* **1974**, *78*, 265.

(10) Mukai, K.; Hara, T.; Ishizu, K. *Bull. Chem. Soc. Jpn.* **1979**, *52*, 1853.

(11) (a) Nishide, H.; Kaneko, T.; Nii, T.; Katoh, K.; Tsuchida, E.; Yamaguchi, K. *J. Am. Chem. Soc.* **1995**, *117*, 548. (b) Nishide, H.; Kaneko, T.; Nii, T.; Katoh, K.; Tsuchida, E.; Lahti, P. M. *J. Am. Chem. Soc.* **1996**, *118*, 9695. (c) Nishide, H.; Miyasaka, M.; Tsuchida, E. *Angew. Chem., Int. Ed. Engl.* **1998**, *37*, 2400. (d) Nishide, H.; Miyasaka, M.; Tsuchida, E. *J. Org. Chem.* **1998**, *63*, 7399. (e) Nishide, H.; Maeda, T.; Oyaizu, K.; Tsuchida, E. *J. Org. Chem.* **1999**, *64*, 7129. (f) Nishide, H.; Takahashi, M.; Takashima, J.; Pu, Y.-J.; Tsuchida, E. *J. Org. Chem.* **1999**, *64*, 7375.

10.1021/jo0013204 CCC: $20.00
Published on Web 02/10/2001

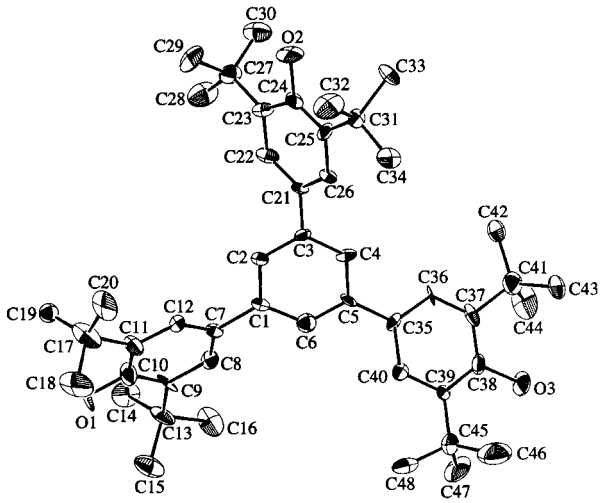

Figure 1. ORTEP view (30% probability ellipsoids) of **1b**.

action in the 1,3,5-benzenetriyltrisphenoxyl molecule have not been elucidated.

In this paper, we reexamine the preparative route of **1b** and first describe the molecular structure of **1b**, the electrochemical behavior of the trisphenoxyl radicals **1a**, and its magnetic susceptibility and magnetization measurements.

Results and Discussion

Synthesis and Crystal Structure of 1b. Our synthesis of **1b** hinged on the use of 1,3,5-tribromobenzene obtained from 2,4,6-tribromoaniline as a core of the molecule. 1,3,5-Tribromobenzene was cross-coupled using a nickel catalyst with [3,5-di-*tert*-butyl-4-(trimethylsiloxy)phenyl]magnesium bromide which was derived from 4-bromo-3,5-di-*tert*-butylphenol (for details, see the Experimental Section). The total yield of **1b** was more than 10%, which was significantly improved from that of Zimmermann's method[8] (trace) using the HCl condensation of 4-acetyl-2,6-di-*tert*-butylphenol.

The triphenol **1b** was isolated as colorless platelike crystals. The crystal structure (Figure 1) was determined by an X-ray crystallographic analysis, which revealed that eight molecules were involved in a monoclinic cell. The molecule occupies a general equivalent position with no crystallographic site symmetry but appears to consist of 3-fold rotational symmetry. The propeller-like shape of three chemically equivalent hydroxyphenyl groups is clearly apparent when the molecule is viewed along the approximate 3-fold axis that passes through the central benzene core. The dihedral angles between the peripheral hydroxyphenyl groups and the central benzene core adhere reasonably closely to the C_3 symmetry. The three peripheral groups are twisted from the central core by 33.8, 45.6, and 38.2°, respectively. The C_3-symmetric structure and the fairly planar conformation are reflected in the properties of the 1,3,5-triphenylbenzene unit as a π-conjugated redox and magnetic coupler (vide infra).

Radical Formation and Its Electrochemistry. 2,4,6-Tris-*tert*-butylphenolate undergoes a one-electron oxidation to the corresponding phenoxyl radical at 0.34 V.[11b] The reversible oxidation and reduction wave couple in the cyclic voltammograms of **1b** and **2b** in the basic solution (Figure 2) corroborates the persistency of the phenoxyl radicals, **1** and **2**, in the electrolyte solution at room temperature.

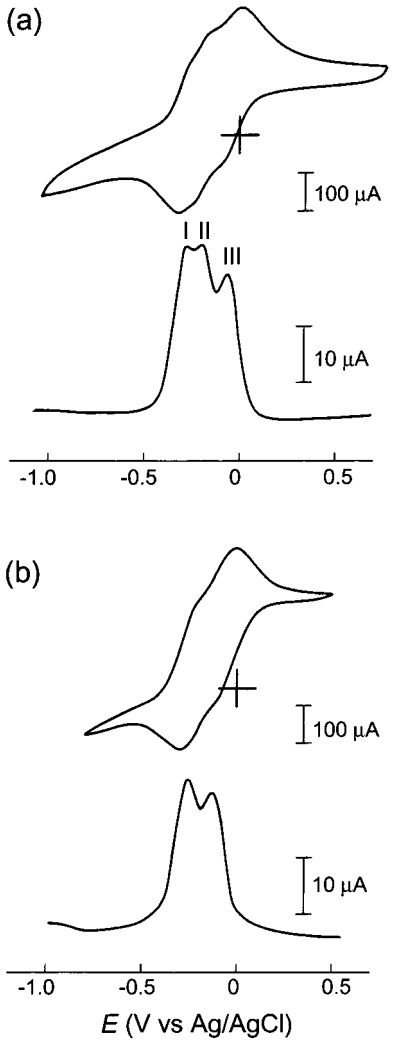

Figure 2. Cyclic and differential pulse voltammograms for a 0.5 mM solution of (a) **1b** and (b) **2b** in anaerobic anhydrous dichloromethane containing 0.1 M tetrabutylammonium tetrafluoroborate and 8 equiv of tetrabutylammonium hydroxide (10% methanol solution). Cyclic voltammetry: scan rate = 100 mV/s. Differential pulse voltammetry: scan rate = 1 mV/s, pulse amplitude = 50 mV, width = 5 ms.

The oxidation of multiple, electrochemically equivalent phenolate groups combined with one polymer chain provided only a statistical mixture of polyradicals according to the oxidation state.[11b] On the other hand, the oxidation of the triphenol **1b** is expected to provide the discrete radical at each oxidation state. The cyclic and differential pulse voltammograms of **1b** recorded under the basic conditions revealed a three-wave profile labeled **I**, **II**, and **III** in Figure 2a. Throughout the experiments, the oxidation of **1b** was performed in the presence of a sufficient amount of tetrabutylammonium hydroxide so that the redox response corresponded to that of the triphenolate anion. Controlled potential electrolysis using a large-area carbon felt electrode maintained at 0.5 V resulted in transfer of 3 electrons per molecule of **1b**. The spin concentration of the electrolyzed solution amounted to 2.9 spins per molecule of **1b**, which was determined by the integration of the ESR signal recorded in the electrolytic ESR spectroscopy. Accordingly, the waves **I-III** are to be assigned to the redox process of the three phenolate groups as shown in Scheme 1.

Scheme 1

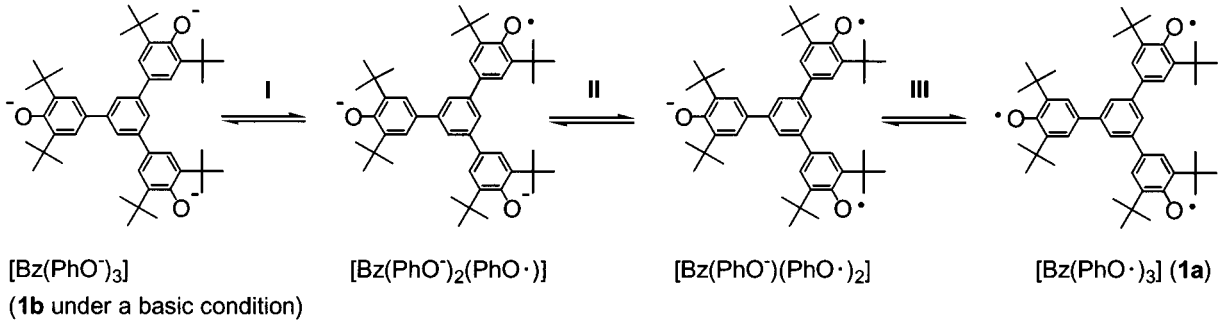

Table 1. Electrochemical Data for the Oxidation of the Triphenol 1b and the Diphenol 2b under the Basic Conditions[a]

half reaction		E_{pa}[b]	E_{pc}[c]	$E_{1/2}$[d]	E_p[e]
$[Bz(PhO^-)_3]$ (**1b**) → $[Bz(PhO^-)_2(PhO^·)] + e^-$	(**I**)	−0.32[f]	−0.38	−0.35	−0.34
$[Bz(PhO^-)_2(PhO^·)] → [Bz(PhO^-)(PhO^·)_2] + e^-$	(**II**)	−0.22	−0.29[f]	−0.26	−0.27
$[Bz(PhO^-)(PhO^·)_2] → [Bz(PhO^·)_3]$ (**1a**) $+ e^-$	(**III**)	−0.04	−0.14[f]	−0.09	−0.12
$[Bz(PhO^-)_2]$ (**2b**) → $[Bz(PhO^-)(PhO^·)] + e^-$		−0.30[f]	−0.36	−0.33	−0.32
$[Bz(PhO^-)(PhO^·)] → [Bz(PhO^·)_2]$ (**2a**) $+ e^-$		−0.07	−0.16[f]	−0.12	−0.20

[a] Concentration = 0.5 mM, solvent = CH_2Cl_2, supporting electrolyte = 0.1 M $(C_4H_9)_4NBF_4$ + 4 mM $(C_4H_9)_4NOH$. [b] Oxidation peak potential in V vs Ag/AgCl determined by cyclic voltammetry. Ferrocene/ferrocenium redox couple was at 0.33 vs this Ag/AgCl. [c] Reduction peak potential. [d] $(E_{pa} + E_{pc})/2$. [e] Peak potential in V vs Ag/AgCl determined by differential pulse voltammetry. Scan rate = 1 mV/s, pulse amplitude = 50 mV, width = 5 ms. [f] Not resolved.

Added support has been provided using the diphenol **2b** which undergoes two successive reversible one-electron oxidations to yield the mono- and diradicals (Figure 2b). The controlled potential electrolysis of **2b** at 0.5 V consumed two electrons per molecule of **2b** in accordance with the number of the phenolate site. The coulometric titration experiments also support the absence of fragmentation or side reactions during the oxidation. The electrochemical data for **1b** and **2b** are summarized in Table 1.

The π-conjugated but non-Kekulé-type structures of **1a** and **2a** exclude a quinoid formation or a two-electron transfer reaction and realize the sequence of one-electron transfer reactions. It is considered that because of the intramolecular interactions between the phenolate groups, the initial one-electron oxidation renders the subsequent oxidation energetically less favorable. Therefore, the subsequent oxidation occurs at a higher potential, resulting in the stepwise current−potential curve as demonstrated in Figure 2. It should be noted that the second oxidation potential of **1b** is slightly lower than that of **2b** as a result of an electron-donating effect and/or an electrostatic effect of the extra phenolate group. An estimate of the extent of the phenolate-phenolate interactions is obtained from the value of the comproportionation constants, $K_c(1)$ and $K_c(2)$, for equilibria 1 and 2, respectively.

$$[Bz(PhO^-)_3] + [Bz(PhO^-)(PhO^·)_2] \overset{K_c(1)}{\rightleftharpoons} 2[Bz(PhO^-)_2(PhO^·)] \quad (1)$$

$$[Bz(PhO^-)_2(PhO^·)] + [Bz(PhO^·)_3] \overset{K_c(2)}{\rightleftharpoons} 2[Bz(PhO^-)(PhO^·)_2] \quad (2)$$

The values of $K_c(1)$ and $K_c(2)$ are related to the extent of redox couplings; the separations between the three consecutive redox potentials, $\Delta E^f(1) = E^f(\mathbf{II}) - E^f(\mathbf{I})$ and $\Delta E^f(2) = E^f(\mathbf{III}) - E^f(\mathbf{II})$, by the expression, $\ln K_c = F\Delta E^f/RT$. Waves **I**−**III** are well resolved by differential pulse voltammetry. The values of $\Delta E_p(1) = E_p(\mathbf{II}) - E_p(\mathbf{I})$ and $\Delta E_p(2) = E_p(\mathbf{III}) - E_p(\mathbf{II})$, due to the electrochemically reversible nature of the process, approximates $\Delta E^f(1)$ and $\Delta E^f(2)$, respectively. The equilibrium constants are determined to be $K_c(1) = 15$ and $K_c(2) = 340$.

The large value of $K_c(2)$ indicates that the diradical of **1b** substantially persists in solution. This is not contradictory to the previous study describing that the oxidative titration of **2b** with PbO_2 affords the monoradical which can be detected by ESR as a sole species in the solution.[10] Indeed, the comproprotionation constant for the generation of the monoradical of **2b** is determined to be 107 from the extent of the redox coupling. On the contrary, the value of $K_c(1)$ suggests that the monoradical of **1b** can be generated up to only 66% of the total amount of the molecule in the equilibrated solution (Figure 3).

The triradical **1a** can be obtained not only by electrolytic oxidation but also by a chemical oxidation such as a heterogeneous oxidation with aqueous ferricyanide. A more convenient method for the preparation of the diradical of **1b** is the combination of solutions of the triphenolate and the electrochemically prepared triradical **1a** in the molar ratio of 1:2. The pure monoradical could not be obtained even by mixing the triphenolate and **1a** in a 2:1 ratio due to the concomitant disproportionation reaction (eq 1), which produced the equilibrium mixture with the composition of triphenolate/monoradical/diradical = 17:66:17 (Figure 3). In attempts to obtain the monoradical with a lower amount of the diradical, the ferricyanide titration of **1b** was employed to obtain a solution with a spin concentration of slightly less than 1 per molecule. For example, a spin concentration of 0.89 per molecule corresponds to the equilibrated solution with the composition of triphenolate/monoradical/diradical/triradical = 23:65:12:0. The disproportionation of the monoradical is reflected in the upward deviation of $\chi_{mol}T$ at low spin concentrations from the value expected for the pure monoradical solution (vide infra).

ESR Spectra. The stepwise oxidation of the triphenolate is also evidenced by the ESR spectra of the electrolytically resulting radicals as shown in Figure 4, which

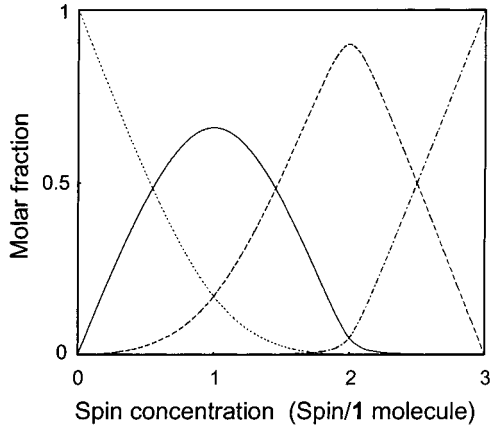

Figure 3. Molar fraction profile of **1b** under a basic condition (···), the monoradical (—), the biradical (- - -), and the triradical **1a** (-·-·-) equilibrated at each spin concentration. The molar fraction of each species in the equilibrated solution can be determined as a function of the spin concentration by the following equations: $[\text{monoradical}]^2/([\mathbf{1b}][\text{biradical}]) = 15$, $[\text{biradical}]^2/([\text{monoradical}][\mathbf{1a}]) = 340$, $[\mathbf{1b}] + [\text{monoradical}] + [\text{biradical}] + [\mathbf{1a}] = 1$, spin concentration $= 1 \times [\text{monoradical}] + 2 \times [\text{biradical}] + 3 \times [\mathbf{1a}]$.

provide an insight into the magnetic coupling through the 1,3,5-benzenetriyl core. The ESR spectrum of the radical with low spin concentration (Figure 4a) is reasonably ascribed to the signal of the phenoxyl radical, which revealed a six-line hyperfine structure with the intensity ratio of 1:5:10:10:5:1 due to the five equivalent protons (two protons of the phenoxyl ring and three protons of the benzene core). The hyperfine coupling constant a_H was estimated by spectral simulation to be 0.171 mT, which agreed with the previously reported coupling constant for the phenoxyl radical with the similar structures.[8,10] These results suggest an effective distribution of spin density of the phenoxyl's unpaired electron over the benzenetriyl core.

The ESR spectrum of the diradical of **1b** gave a broad hyperfine structure due to the unresolved coupling of the 5 protons (Figure 4b). The ESR spectra showed sharp and unimodal signals with increasing spin concentration and for the triradical **1a** (Figure 4c), indicating a locally high spin concentration within the molecule.

The frozen toluene glass of a 10 mM **1a** (formed by the chemical oxidation) gave a $\Delta M_s = \pm 2$ forbidden transition ascribed to a triplet species at $g = 4$ (inset in Figure 5). The ESR signal in the $\Delta M_s = \pm 2$ region was doubly integrated by varying the temperature to give Curie plots (Figure 5). Although the signal intensity is proportional to the reciprocal of the absolute temperature ($1/T$) at high temperature, the plots substantially deviate upward from linearity in the lower temperature region. This upward deviation suggests increased population of the triplet and/or quartet ground states in the low temperature and a ferromagnetic interaction between the phenoxyl spins. A quartet species was not detected in the ESR spectrum probably due to the very small transition moment for $\Delta M_s = \pm 3$. Control experiments using the diradical **2a** also revealed the presence of the triplet state. The signal intensity of the $\Delta M_s = \pm 2$ transition for **2a** was roughly one-third of that for **1a** (Figure 5), in accordance with the number of possible triplet states. Smaller upward deviation of the signal intensity for **2a** than for **1a** suggested a strong ferromagnetic interaction for **1a**.

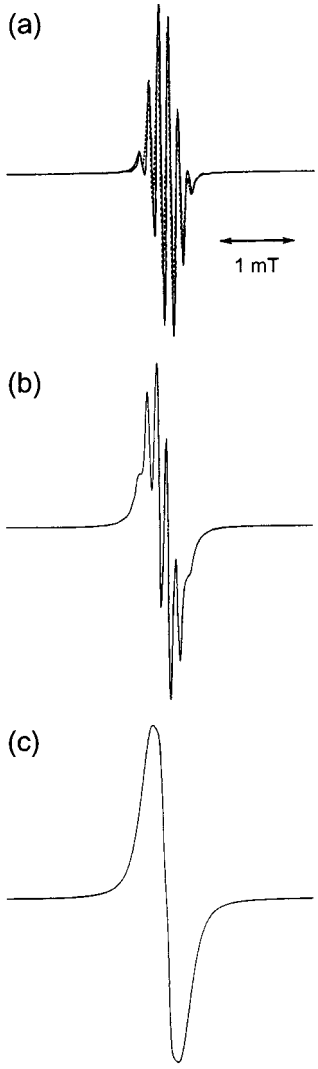

Figure 4. ESR spectra of the radicals electrolytically derived from **1b** (0.25 mM) in benzene: (a) the solid curve for the monoradical of **1b** (0.19 spin/molecule) and the dashed curve for the simulated best-fit spectrum ($a_H = 0.171$ mT); (b) the diradical of **1b** (2.0 spin/molecule); (c) the triradical **1a** (spin concn = 2.9 spin/molecule).

Magnetic Properties. Static magnetic susceptibility and magnetization of the radicals derived from **1b** by the chemical oxidation were measured with a SQUID magnetometer. The radicals were diluted in diamagnetic toluene to minimize any antiferromagnetic and intermolecular interactions. The plots of the product of molar magnetic susceptibility (χ_{mol}) and T vs T are shown in Figure 6. They decreased at lower temperature (<10 K), indicating an antiferromagnetic (probably a through-space between the radical molecules) interaction even under these conditions. The values of $\chi_{mol}T$ clearly increased with the spin concentration, and approached the theoretical value for $S = 3/2$ ($\chi_{mol}T = 0.625$ emu·K/mol) and 2/2 (0.500), for the radical with a spin concentration of 2.89 (or almost the triradical **1a**) and the radical with a spin concentration of 2.00 (or the diradical), respectively.[12] The $\chi_{mol}T$ value for the monoradical solution (spin concentration = 0.89) was somewhat larger than the theoretical value for $S = 1/2$ ($\chi_{mol}T = 0.375$ emu·

(12) Here, χ_{mol} is based on per mol of phenoxyl. The spin concentrations estimated from the magetization data at saturation were given in the caption of Figure 7.

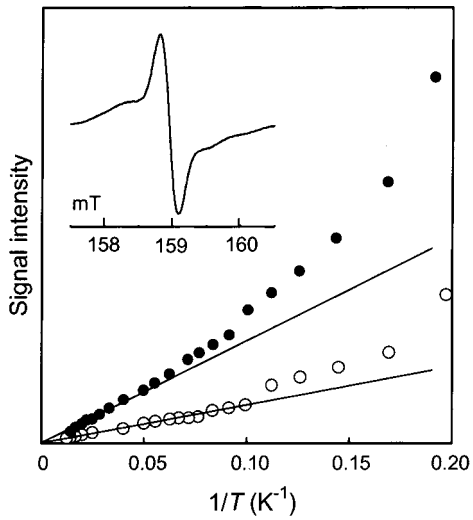

Figure 5. Curie plots for the peak in the $\Delta M_s = \pm 2$ region for the chemically prepared triradical **1a** (●) and diradical **2a** (○) in toluene glass (10 mM) at 6.5 K; inset, $\Delta M_s = \pm 2$ spectrum for **1a**.

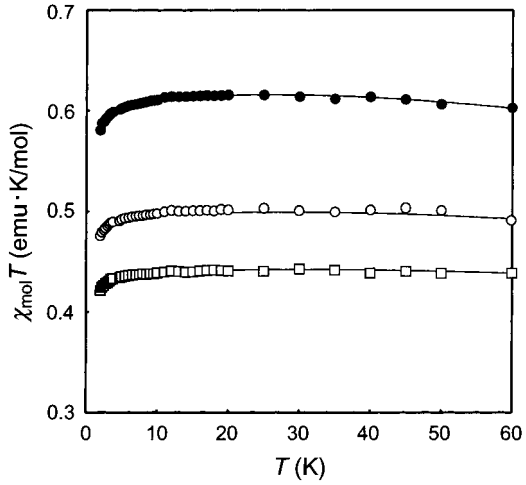

Figure 6. $\chi_{mol}T$ vs T plots of the toluene glass of the radicals derived from **1b** with spin concentration of 2.89 (●), 2.0 (○), and 0.89 (□) spin/molecule. χ_{mol} is based on per mol of phenoxyl.

K/mol), probably as a result of the presence of a small amount of the diradical disproportionated from the monoradical.[13] It should be noted that the $\chi_{mol}T$ plots are flat at the temperature range of 15−60 K, which suggests a strong exchange interaction between the phenoxyl's spins.

The normalized plots of magnetization, M/M_s, of the radicals are plotted vs the effective temperature $(T - \theta)$ and compared with the Brillouin curves (Figure 7), where θ is a coefficient of the weak antiferromagnetic interaction between the radicals and is estimated from curve fitting using the $\chi_{mol}T$ *vs* T data. The disproportionation of the monoradical resulted in the upward deviation of the M/M_s plots from the theoretical Brillouin $S = 1/2$ curve. The M/M_s plots for the diradical close to the $S = 2/2$ curve support a triplet ground state. The M/M_s plots for the triradical **1a** lie almost on the curve for $S = 3/2$, indicating a quartet ground state of the triradical.

(13) The magnitude of the deviation is in agreement with the amount of the monoradical and the diradical equilibrated in the solution with the spin concentration of 0.89. Thus, the composition of monoradical: biradical: triradical = 65:12:0, according to Figure 3, corresponds to the calculated value of $\chi_{mol}T = 0.41$ emu·K/mol.

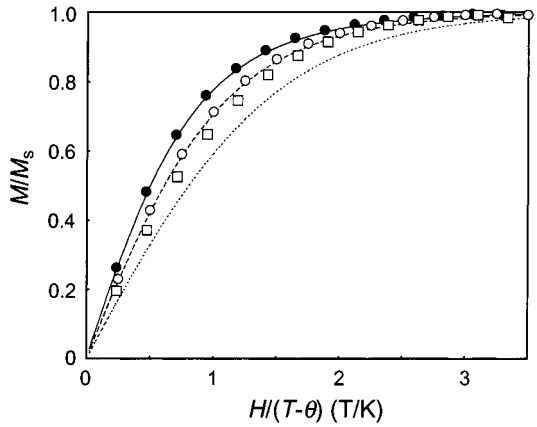

Figure 7. Normalized plots of magnetization (M/M_s) vs the ratio of magnetic field and temperature ($H/(T - \theta)$) for the radicals derived from **1b** with a spin concentration of 2.89 (●), 2.0 (○), and 0.89 (□) spin/molecule (spin concn estimated from the magnetization at saturation = 2.5, 1.8, and 0.8 spin/molecule, and $\theta = -0.19$, -0.12, and -0.17 K, respectively) and the theoretical curves corresponding to the $S = {}^1/_2$, 1, and ${}^3/_2$ Brillouin functions.

Conclusion

The π-conjugated but non-Kekulé-type 1,3,5-benzenetriyl core is an effective coupler between the three phenolate/phenoxyl redox sites in the electron-transfer reaction. The core also acted as a strong ferromagnetic coupler to allow a strong intramolecular through-bond exchange interaction between the unpaired electrons of three phenoxyl radicals attached to the 1,3,5-benzenetriyl positions. Polyradicals composed of 1,3,5-benzenetriyl cores and pendant phenoxyls are expected to display a very high-spin alignment within the polyradical molecules.

Experimental Section

1,3,5-Tris(3′,5′-di-*tert*-butyltrimethylsilylphenyl)benzene. Magnesium powder (5.4 g, 0.224 mol) was dried for 3 h at 120 °C under a nitrogen atmosphere. After cooling, (4-bromo-2,6-di-*tert*-butylphenoxy)trimethylsilane (80.2 g, 0.224 mol) and THF (100 mL) were added and the mixture was refluxed for 8 h. Following the addition of THF (100 mL), the mixture was cooled to room temperature. The mixture was added dropwise to the THF (113 mL) solution of 1,3,5-tribromobenzene (20 g, 0.064 mol) and dichloro[1,3-bis(diphenylphosphino)propane]nickel(I) (0.16 g), and the resulting solution was refluxed for 12 h. The solution was treated with 2 N HCl (71 mL) and neutralized with sodium hydrogencarbonate. The product was extracted with diethyl ether, washed with water, and dried over anhydrous sodium sulfate. After evaporation of the solvent, the crude product was purified by column chromatography on silica gel with hexane/chloroform as an eluent to give 1,3,5-tris(3′,5′-di-*tert*-butyl-trimethylsilylphenyl)-benzene. Yield: 13%. IR (KBr, cm^{-1}): 3038−2874 (ν_{C-H}), 1227 (ν_{Si-C}), 916 (ν_{Si-O}). ^{1}H NMR ($CDCl_3$, 500 MHz, ppm): 0.48 (s, 18H, $-SiCH_3$), 1.51 (s, 36H, −*tert*-butyl), 7.58 (s, 6H, ArH), 7.64 (s, 3H, ArH). ^{13}C NMR ($CDCl_3$, 500 MHz, ppm): 4.75, 30.5, 34.6, 123.5, 124.7, 132.5, 141.2, 143.0, 152.3. Mass: calcd for M 908, found (m/z) 908 (M^+).

1,3,5-Tris(3′,5′-di-*tert*-butylhydroxyphenyl)benzene (1b). 1,3,5-Tris(3′,5′-di-*tert*-butyltrimethylsilylphenyl)benzene (2.0 g, 2.2 mmol) was dissolved in THF (8 mL), and methanol (12 mL) was added to the solution. Under a nitrogen atmosphere, 10 N HCl (4 mL) was added to the solution, and the mixture was stirred for 3 h at room temperature. After evaporation of methanol, the product was extracted with diethyl ether, washed with water, and dried over anhydrous sodium sulfate.

After evaporation of diethyl ether, the crude product was purified using a silica gel column with a chloroform/hexane eluent. Recrystallization from hexane afforded 1,3,5-tris(3′,5′-di-*tert*-butylhydroxyphenyl)benzene as colorless crystals. Yield: 66%. IR (KBr, cm^{-1}): 3641 (ν_{O-H}), 2961−2874 (ν_{C-H}). ^1H NMR ($CDCl_3$, 500 MHz, ppm): 1.53 (s, 36H, -*tert*-butyl), 5.29 (s, 3H, −OH), 7.48 (s, 6H, ArH), 7.58 (s, 3H, ArH). ^{13}C NMR ($CDCl_3$, 500 MHz, ppm): 30.4, 34.5, 124.4, 124.6, 133.1, 136.3, 143.1, 153.6. Mass calcd for M 691, found (*m*/*z*) 691 (M^+). Mp: 313 °C (lit.[8] mp 313−314 °C). UV (ethanol, λ_{max}, nm): 270 (lit.[8] λ_{max} (nm) 271).

Other Materials. *m*-Bis(3′,5′-di-*tert*-butyl-4-hydroxyphenyl)benzene (**2b**) was prepared by the nickel-catalyzed cross coupling of *m*-dibromobenzene and (4-bromo-2,6-di-*tert*-butylphenoxy)trimethylsilane and was characterized as previously reported.[10] 1,3,5-Tribromobenzene was prepared by reduction of 2,4,6-tribromoaniline. All solvents were purified by distillation. Tetrabutylammonium tetrafluoroborate and potassium ferricyanide were purified by recrystallization. All other reagents were used as received.

Oxidation. Aqueous solutions of excess sodium hydroxide and potassium ferricyanide were successively added to a toluene solution of the hydroxy precursor **1b** (0.25 mM) with vigorous stirring at room temperature in a glovebox. The color of the organic layer changed from purple to deep violet, and finally to orange-brown, according to the spin concentration. After the mixture was stirred for 30 min, the organic layer was separated, washed with water, and dried over anhydrous sodium sulfate to give the radical solution.

ESR and SQUID Measurements. ESR spectra were taken using a JEOL TE−200 spectrometer with a 100 kHz field modulation. The spin concentration of each sample was determined both by careful integration of the ESR signal standardized with that of 2,2,6,6-tetramethyl-1-piperidinyloxyl solution and by analyzing the saturated magnetization in the SQUID measurement.

The toluene solution of the radical (5 mM) was immediately transferred to a diamagnetic capsule after the oxidation. Magnetization and static magnetic susceptibility were measured with a Quantum Design MPMS-7 SQUID magnetometer. The static magnetic susceptibility was measured from 1.8 to 200 K at a field of 0.5 T.

Electrochemical Measurements. All measurements were performed in a glovebox under an atmosphere of dry argon. Electrochemical measurements were carried out in a conventional two-compartment cell. A glassy carbon disk-platinum ring was used as a working electrode and polished before each experiment with 0.05-μm alumina paste. The auxiliary electrode, a coiled platinum wire, was separated from the working solution by a fine-porosity frit. The reference electrode was a commercial Ag/AgCl immersed in a salt bridge consisting of a CH_2Cl_2 solution of 0.1 M tetrabutylammonium tetrafluoroborate, which was placed in the main cell compartment. The formal potential of the ferrocene/ferrocenium redox couple was 0.33 V vs this reference electrode. All potentials are quoted with respect to this Ag/AgCl electrode. A BAS 100B/W electrochemical analyzer was employed to obtain the cyclic and differential pulse voltammograms. Coulometric exhaustive electrolysis was performed using a Nikko Keisoku NDCM-1 digital coulometer with a DPGS-1 potentiogalvanostat.

Other Measurements. X-ray crystallographic analysis was made on a Rigaku AFC7R diffractometer (see Supporting Information). ^1H and ^{13}C NMR, infrared, and FABMS spectra were obtained using a JEOL Lambda 500 spectrometer, a JASCO FT-IR 5300 with potassium bromide pellets, and a VGZAB-HF spectrometer, respectively.

Acknowledgment. This work was partially supported by Grants-in-Aid for Scientific Research Nos. 09305060 and 12555268 from the Ministry of Education, Science and Culture, Japan.

Supporting Information Available: Details of crystallographic analysis including tables giving bond lengths and angles, atomic coordinates, equivalent isotropic thermal parameters, and anisotropic displacement parameters for **1b**. This material is available free of charge via the Internet at http://pubs.acs.org.

JO0013204